Spontaneous formation of nanometric multilayers of metal-carbon films by up-hill diffusion during growth

C. Corbella
FEMAN, Departament de Física Aplicada i Òptica, Universitat de Barcelona, c/ Martí i Franquès 1, E-08028, Barcelona, Spain

B. Echebarria and L. Ramírez-Piscina
Departament de Física Aplicada, Universitat Politècnica de Catalunya, Av. Doctor Marañón 44, E-08028, Barcelona, Spain

E. Pascual,[a] J. L. Andújar, and E. Bertran
FEMAN, Departament de Física Aplicada i Òptica, Universitat de Barcelona, c/ Martí i Franquès 1, E-08028, Barcelona, Spain

(Received 14 July 2005; accepted 27 September 2005; published online 18 November 2005)

We report the spontaneous formation of multilayer structures with nanometric periodicity during Ti–C thin-film growth by reactive magnetron sputtering. Their characterization was performed by transmission electron microscopy, x-ray photoelectron spectroscopy, x-ray diffraction, and secondary ion mass spectrometry. We discuss film structure and morphology as a function of metal content, and propose surface-directed spinodal decomposition as the mechanism responsible for the segregation of species in separated layers by up-hill diffusion. © *2005 American Institute of Physics*. [DOI: 10.1063/1.2135385]

Nanostructured thin films offer novel opportunities for the design of materials with new or enhanced properties. Preparation of smart films for their performance as protective hard coatings is an important issue of material engineering.[1] Multilayers,[2] composition grading,[3] and nanocomposites[4] of hard constituents can lead to coatings with superior mechanical properties, specially addressed to magnetic storage devices, cutting tools, and biomedical implants. Combination of metals and diamondlike carbon into metal-carbon (Me–C) films has provided excellent results since their initial study two decades ago.[5–7] A self-organized multilayer structure is then expected to introduce an intrinsic improvement of their hardness, mechanical consistency, and wear resistance. Indeed, spontaneous nanostructuring in Me–C thin films is an interesting possibility, since often equilibrium phase diagrams present wide ranges of metal content and temperature in which homogeneous phases are thermodynamically unstable. Annealing of films grown inside such a miscibility gap can enhance up-hill diffusion, and hence facilitate segregation.[8,9] But already during film growth, the deposited atoms dispose of an excess of energy to diffuse, which is subject to being experimentally controlled. Furthermore, the intrinsic anisotropy of the growth process, together with its nonequilibrium character, may induce nontrivial morphological effects at segregation scales.

In this work, we have explored this possibility for the Ti–C system, whose equilibrium miscibility gap spans from 0 to 50 at. % Ti for temperatures below 3049 K. Ti–C thin films were deposited by pulsed-dc reactive magnetron sputtering of a Ti target in an Ar-diluted CH_4 atmosphere.[7] The substrates consisted of monocrystalline Si (100) wafers, which were placed on a sample holder biased by means of radio frequency (13.56 MHz) to −200 V in order to increase the ion bombardment. The target cathode was driven by an asymmetrical bipolar pulsed-dc power supply (ENI RPG-50). The consigned values were 100 W, 100 kHz pulse frequency, and 70% duty cycle. Ar and CH_4 were injected at a total gas flow of 40 sccm. Ti content was controlled by the relative CH_4 flow ratio, R, which was varied from 0 to 25% and the gas pressure was 5 Pa. A rapid quench of the deposited species was induced by maintaining samples at room temperature.

A thorough characterization of film structure was performed by several techniques: Transmission electron microscopy (TEM), x-ray photoelectron spectroscopy (XPS), x-ray diffraction (XRD), and secondary ion mass spectrometry (SIMS). The chemical composition was calculated from XPS analysis using a Perkin–Elmer PHI 5500 spectrometer. Samples prepared with R equal to 0, 2, 3, 6, and 25% yielded a composition of 100, 60, 25, 5, and nearly 0 at. % Ti, respectively. An Atomika A-DIDA 3000-30 spectrometer was employed for SIMS measurements. Cross-section TEM micrographs and selected area electron diffraction (SAED) patterns were obtained by a Philips CM30 electron microscope operated at an accelerating voltage of 300 kV. High-resolution TEM (HRTEM) images and electron energy loss spectroscopy (EELS) composition mappings were provided by an electron microscope working at 200 kV which is equipped by a JEOL Jem 2010F field emission gun. XRD measurements were performed by a Siemens D-500 x-ray diffractometer. Films thicknesses were measured with a Dektak 3030 surface profilometer. The mechanical residual stress was determined by measuring the radius of curvature of the substrate, before and after the deposition, and applying Stoney's equation.

Figure 1 shows cross-section TEM micrographs and SAED spectra corresponding to Ti–C films prepared at R values of 2, 3, and 6%. Their growth rates were 0.018, 0.040, and 0.045 nm/s, respectively. A multilayer nanostructure is inferred from the plano-parallel alternating contrast modulation. The first layer after the substrate is the thickest one,

[a]Author to whom correspondence should be addressed; electronic mail: epascual@ub.edu

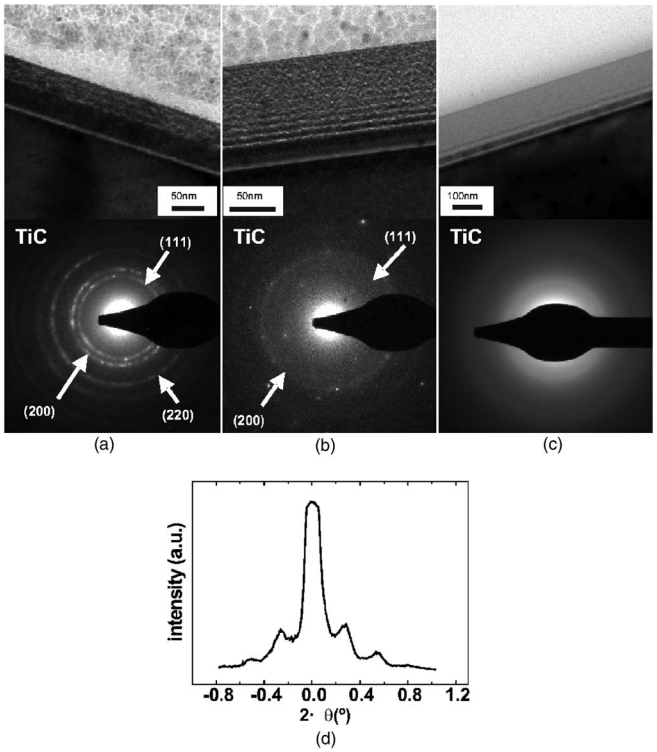

FIG. 1. Cross-section TEM micrographs of Ti–C films with: 60 at. % Ti (a), 25 at. % Ti (b), and 5 at. % Ti (c). The corresponding SAED patterns are located below each image. The compositional modulation is evidenced by the superlattice electron diffraction spectrum of the sample with 25 at. % Ti (d).

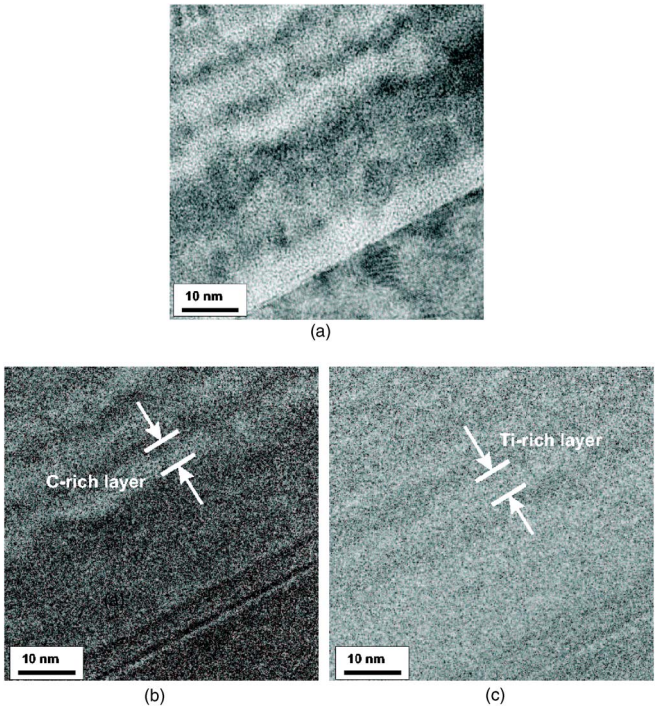

FIG. 2. TEM image showing multilayer structure of a Ti–C film with 25 at. % Ti (a). EELS mappings of the same region highlight C-rich (b) and Ti-rich (c) layers.

probably revealing the affinity of the substrate to one of the components. Furthermore, the modulation is lost in the outmost layers, where material mixing may occur. In the extreme case, the C-richest sample ($R=25\%$) consisted of a C film stacked onto a thin Ti-rich interlayer, as revealed by depth-profile composition analysis by SIMS. Compositional mappings in a region from the sample with 25 at. % Ti [Fig. 2(a)] were obtained by means of EELS analysis. Ti and C signals appear alternatively arranged in layers, as displayed in Figs. 2(b) and 2(c), indicating a diffused compositional modulation throughout the film. The periodicity of the multilayer was measured using SAED. This provided a superlattice diffraction spectrum, whose profile is shown in Fig. 1(d). An average bilayer period of 8.2 nm was calculated, which is consistent with the micrographs in Fig. 1.

During film growth, the deposition energy of the atoms enhances diffusivity near the growing surface of the film by many orders of magnitude.[10–12] We propose that the bands observed at 60, 25, and 5 at. %. Ti appear in a nonequilibrium process, through the mechanism of spinodal decomposition in this external layer. There, atomic interactions that favor atoms of the same species overcome the tendency to maximize entropy, producing up-hill diffusion. Then, an initially thermodynamically unstable concentration of Ti–C develops spatial modulations, segregating into Ti- and C-rich amorphous phases. Contrary to nucleation, spinodal decomposition induces segregation through compositional modulations of a well-defined wavelength.[13]

We have tested this scenario by numerical simulations of a modified version of the Cahn–Hilliard model of phase separation.[14] The basic ingredients of this model are the species diffusivity, and the bulk and interfacial free energies. From the concentration of carbon, we define a new variable $u=(2c-c_\beta-c_\alpha)/(c_\beta-c_\alpha)$, where c_α and c_β are the carbon concentrations in the Ti-rich and C-rich metastable amorphous states. The evolution of this variable obeys a conservation equation $\partial_t u=-\nabla\cdot\mathbf{j}$, with the flux $\mathbf{j}=D(1-\phi^2)\nabla\mu$ taking negligible values except in a region of width ℓ_D near the surface, where the atoms have enough energy to diffuse. This is enforced defining a field $\phi=\tanh[(z-v_{fg}t)/\ell_D]$, that separates the film ($\phi=-1$), where material has been deposited, from the plasma ($\phi=1$), with a diffuse interface of width $\sim\ell_D$. The film surface grows with velocity v_{fg}, that depends on the deposition rate. The chemical potential of the binary system $\mu=u-u^3+\kappa^2\nabla^2u+V(z)$ has minima corresponding to the two metastable states ($c=c_\alpha$ and $c=c_\beta$), a term accounting for the interfacial energy (κ being the gradient energy coefficient), and a potential $V(z)=h_1$, for $z<z_0$ and $V(z)=h_1z_0^2/z^2$, for $z>z_0$, that incorporates the larger affinity of the substrate for one of the components.[15] We consider that the deposited concentration fluctuates around an average value, $u=u_0+\xi(\mathbf{r})$, with $\langle\xi(\mathbf{r}'),\xi(\mathbf{r})\rangle=\sigma^2\delta(\mathbf{r}'-\mathbf{r})$.

The wavelength of the developing segregation pattern, λ_{sp}, is given solely by the ratio between the curvature of the free energy curve at the given initial concentration, and the interfacial gradient coefficient. Together with the diffusivity, these parameters also provide the time scale in which the bands appear. Results show that the interaction with the substrate, which acts during the early stages of film growth, together with the inherent periodicity of the spinodal decomposition process, are enough for coherent formation of the successive layers. Simulation patterns obtained for increasing values of C concentration are shown in Figs. 3(a)–3(c) in a case with large growth velocity v_{fg}. The initial segregation induced by the presence of the substrate is more effective for concentrations in the middle of the miscibility gap, but is only able to form a few layers during a small transient, since

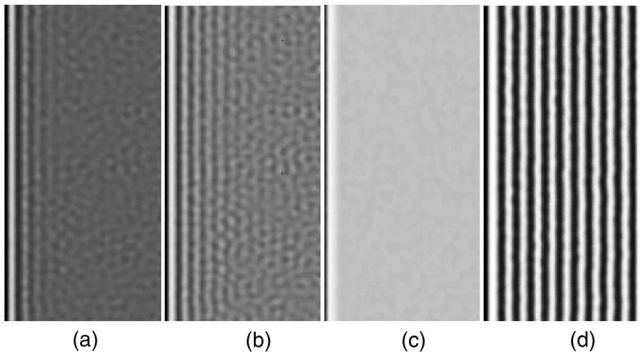

FIG. 3. Simulation patterns of Ti–C multilayers generated with the Cahn–Hilliard model for phase separation. The equations have been solved with an explicit scheme and assuming nonflux boundary conditions, in a box $L_z \times L_x = 40 \times 80$. The effects of changing the concentration and growth velocity on film banding are shown (with dark and light bands corresponding to Ti- and C-rich regions, respectively). The concentration is (a) $u_0 = -0.2$, (b) $u_0 = 0$, (c) $u_0 = 0.4$, with a growth velocity $v_{fg} = 0.6$, and (d) $u_0 = 0$, with a slower growth velocity $v_{fg} = 0.3$. For the other nondimensional parameters, we take $\kappa^2 = 0.4$, $l_D = 2$, $h_1 = -1$, $z_0 = 4$, $D = 0.5$, and $\sigma = 0.2$.

the time during which diffusion is enabled at a given point ($t \sim \ell_D / v_{fg}$) is shorter than the time scale for segregation. By reducing the growth speed, almost perfect bands are produced [Fig. 3(d)].

After segregation, formation of Ti–C crystallites occurs in the Ti-rich layer through nucleation and growth. Three diffraction rings were detected from SAED spectra corresponding to the sample with 60 at. % Ti, indicating that this film lodges randomly oriented TiC crystallites (Fig. 1), which belong to a cubic system, and are labelled as (111), (200), and (220). The lattice parameter is 0.45 nm, as computed using Bragg's law with appropriate software.[16] Film with 25 at. % Ti showed less intense diffraction maxima, and the sample with 5 at. % Ti exhibited a diffuse ring, indicative of its amorphous character. Hence, SAED patterns showed an evolution from a polycrystalline to amorphous state as the metal content in Ti–C films decreased. These results were reproduced in data extracted from XRD measurements. A crystallite's average diameter of about 3.5 nm was obtained for films with both 60 and 25 at. % Ti. The dimension and distribution of crystallites were observed by HRTEM.

Due to the highly cross-linked amorphous matrix of C films with diamondlike properties, Ti–C samples exhibit intrinsic compressive stress, which is found to depend on the composition of the films.[7] In our case, the mechanical stress of Ti–C is a function of Ti content and shows an absolute minimum of −0.9 GPa for 25 at. % Ti, a factor of 3 smaller with respect to pure Ti and C films. Such relaxation in a film structure improves its consistency and substrate adherence, thus diminishing the risk of delamination. This stress reduction seems to be associated with the spontaneous formation of interfaces between the components. This assumption is consistent with the relaxing effect observed in Me–C multilayered films.[17]

In summary, Ti–C films with intermediate metal abundances are observed to spontaneously form multilayers with a nanometric bilayer periodicity. Changes in composition lead to a varying structure, in such a way that the amorphous character of the samples is enhanced as the metal content decreases. A scenario of phase segregation induced by spinodal decomposition explains in a qualitative way the formation of Ti–C multilayered nanostructures. However, additional physical data of the constituents are required to complete this modeling. This spontaneous arrangement in multilayers seems to promote beneficial effects on the mechanical properties of the films.

This study was partially supported by the *Generalitat de Catalunya* (Project Nos. 2001/SGR/00078 and 2001/SGR/00221), and the *CICYT* (Project Nos. MAT2002-04263-C04, MAT2003-02997, BFM2003-07850-C03-02, and FIS2004-02570). The authors thank Serveis Cientificotècnics (SCT) of the Universitat de Barcelona for measurement facilities. Two of the authors (C.C. and B.E.) acknowledge financial support from M.E.C. (Spain).

[1] J. S. Zabinski and A. A. Voevodin, J. Vac. Sci. Technol. A **16**, 1890 (1998).
[2] P. E. Hovsepian, D. B. Lewis, and W.–D. Münz, Surf. Coat. Technol. **133**, 166 (2000).
[3] S. Zhang, X. L. Bui, Y. Fu, D. L. Butler, and H. Du, Diamond Relat. Mater. **13**, 867 (2004).
[4] K. I. Schiffmann, M. Fryda, G. Goerigk, R. Lauer, P. Hinze, and A. Bulack, Thin Solid Films **347**, 60 (1999).
[5] H. Dimigen, H. Hubsch, and R. Memming, Appl. Phys. Lett. **50**, 1056 (1987).
[6] R. Gåhlin, M. Larsson, and P. Hedenqvist, Wear **249**, 302 (2001).
[7] C. Corbella, M. Vives, A. Pinyol, E. Bertran, C. Canal, M. C. Polo, and J. L. Andújar, Surf. Coat. Technol. **177**, 409 (2004).
[8] H. Kim and P. C. McIntyre, J. Appl. Phys. **92**, 5094 (2002).
[9] O. Knotek and A. Barimani, Thin Solid Films **174**, 51 (1989).
[10] I. Dahan, U. Admon, N. Frage, J. Sariel, and M. P. Dariel, Thin Solid Films **377**, 687 (2000).
[11] H. C. Swart, A. J. Jonker, C. H. Claassens, R. Chen, L. A. Venter, P. Ramoshebe, E. Wurth, J. J. Terblans, and W. D. Roos, Appl. Surf. Sci. **205**, 231 (2003).
[12] C. Arvieu, J. P. Manaud, and J. M. Quenisset, J. Alloys Compd. **368**, 116 (2004).
[13] J. W. Cahn, Trans. Metall. Soc. AIME **242**, 166 (1968).
[14] J. W. Cahn and J. E. Hilliard, J. Chem. Phys. **28**, 258 (1958).
[15] S. Puri and K. Binder, Phys. Rev. E **66**, 061602 (2002).
[16] J. L. Lábár, Microscopy and Analysis **75**, 9 (2002).
[17] E. Bertran, C. Corbella, A. Pinyol, M. Vives, and J. L. Andújar, Diamond Relat. Mater. **12**, 1008 (2003).